

Dynamic testing of unreinforced u-shaped adobe-mudbrick wall unit

B. Samali, D.M. Dowling & J. Li
University of Technology, Sydney, NSW, Australia

ABSTRACT: Traditional adobe (mudbrick) houses are highly susceptible to damage and destruction during seismic events. Vertical corner cracking at the intersection of orthogonal walls is one of the major damage patterns of traditional adobe buildings subject to earthquake forces. There are a number of design and construction features which are considered to be viable means of improving the shear and tearing resistance capacities of corner elements. In order to adequately assess different design improvements a series of tests are being undertaken at the University of Technology, Sydney, Australia. This paper presents the first test in the series: the dynamic shake table testing of an unreinforced u-shaped adobe wall panel (1:2 scale). The paper describes the configuration of the specimen, the development of an appropriate input time history and the resulting damage patterns, which were classic and distinct.

1 INTRODUCTION

The vulnerability of traditional adobe (mudbrick) houses to the force of earthquakes has been known for centuries. The new millennium has included at least ten major earthquakes which have drastically impacted traditional adobe houses, causing tens of thousands of fatalities and impacting hundreds of thousands of people. The recent earthquake in Bam, Iran (M_w 6.6) resulted in at least 43,200 fatalities (USGS, 2004). The vast majority of affected buildings in Bam were made of mudbricks. This earthquake, as well as others in El Salvador, India, Peru, Afghanistan, Iran, Turkey, Mexico and China have heightened the need to address this major global problem. Further research focussing on improving the earthquake resistance of mudbrick dwellings is necessary to reduce losses of both life and livelihood in future seismic events.

2 AIM

The predominant failure pattern of traditional mudbrick houses subject to earthquake loads is vertical cracking at the intersection of orthogonal walls (Zegarra et al, 1997). This corner cracking is the result of shear or tearing failure of bricks and/or the brick-mortar interface in these zones of high stress concentration (Dowling, 2004b). Improvement systems or techniques, which are designed to reduce damage to adobe structures,

should primarily address this main failure pattern. It is thus necessary to develop and refine a means of assessing the performance of wall components, with a focus on the critical corner connections.

The key factors to be considered in the development of a reliable and reproducible experiment include:

- Specimen configuration, dimensions, reinforcement and boundary conditions
- Location of displacement and acceleration instrumentation, and audio-visual equipment
- Shake table input spectra

The experiment described in this paper is the first in a series of dynamic tests of adobe structures being undertaken at the University of Technology, Sydney. Later tests will incorporate different improvement systems and specimen configurations. The main aim of this first experiment was to determine some of the important characteristics relating to the factors described above, such that specimens may be subject to seismic loading which generates common or expected failure patterns. This information forms the framework for future testing to assess the aseismic contribution of different improvement systems, including vertical and horizontal reinforcement (internal and external), pilasters/buttresses, ring beam and roof diaphragm. Supplementary to the assessment of aseismic contribution will be the consideration of the costs and complexity of implementing proposed systems.

3 DESCRIPTION OF SPECIMEN

The specimen tested was a u-shaped wall unit, in 1:2 scale. The dimensions of the specimen are shown in Figure 1. These dimensions satisfy the minimum design criteria for unsupported wall length specified in the adobe supplement to the El Salvador building code (RESESCO, 1997). The specimen consisted of 333 full bricks (150 x 150 x 50 mm) and 56 half bricks (150 x 70 x 50 mm) laid in stretcher bond. The mortar was made of the same mud material as the bricks; all mortar joints were 12 - 13 mm thick. The specimen for this first test was unreinforced. The specimen rested on a concrete base, bonded by a mud mortar bed. The concrete base was connected to steel beams and attached to the shake table.

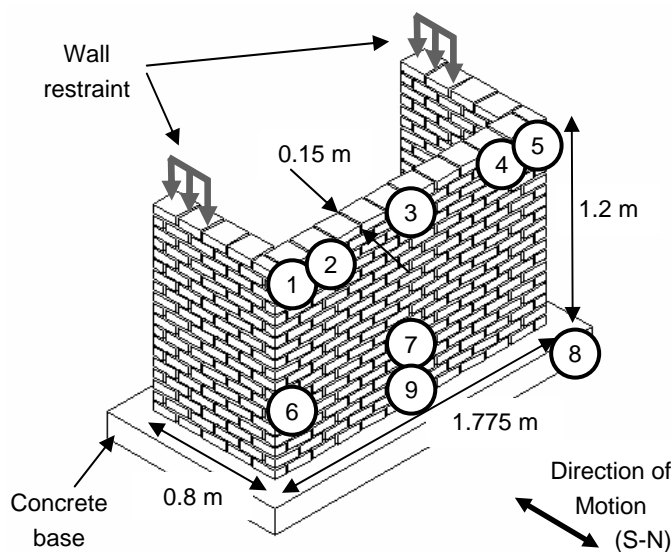


Figure 1. Specimen dimensions and location of LVDT displacement sensors (numbered in circles).

A downward restraining force (Fig. 1) was applied to the tops of the 'wing' walls (acting as in-plane shear walls) to simulate the restraint provided by a continuous wall, and to prevent overturning of the complete unit. This effectively transferred the bulk of the seismic loading to the areas of main interest: the vulnerable out-of-plane long wall, and the corner connections. The restraining force was applied by tension bars between timber platens and beam resting on the walls and the concrete base. A pressure of ~125 kPa was applied, representing 50% of the load which induced initial cracking in a series of compression tests on mudbrick masonry prisms. This applied restraining force is a significant difference between this experiment and other dynamic tests on u-

shaped adobe wall panels, which do not include any 'wing' wall restraint (e.g. Zegarra et al, 1997).

In such cases, the additional stiffness and restraint contributed by the shear walls ('wing' walls) is neglected, which seldom occurs in real structures. This experiment aims to incorporate the contribution of all shear walls in the dynamic response of the system.

For this first specimen no roof load was applied, representing non-load bearing walls, which are common in post-and-beam houses, as well as garden walls and the like. Furthermore, the absence of roof load will somewhat simplify the future task of developing a reliable finite element model, which is regarded as a particularly challenging task due to the inherent variability of both brick and mortar material properties and interactions. Future tests will include a roof load, as well as considering the effects of a roof diaphragm.

4 DESCRIPTION OF EQUIPMENT

The locations of the displacement sensors used in the experiment are shown in Figure 1. The anticipated failure pattern was vertical corner cracking, but it was unknown whether this would be due to shear failure (with cracking in the face of the long wall) or tearing failure (with cracking in the face of the 'wing' walls). In order to record the relative movements for both possibilities, five dynamic LVDTs were placed across the long wall, 80 mm below the top of the wall. A further two dynamic LVDTs were placed 350 mm up from the base, and one dynamic LVDT was located on the concrete base to record the reference base displacement. A single static LVDT was positioned at the mid-point and base of the wall to record the relative displacement of the specimen with respect to the concrete base.

Data for these sensors was recorded on both a PC-based digital data acquisition system, and two analogue Yokogawa dynamic signal analysing recorders.

The dynamic simulation was done on the state-of-the-art MTS uni-axial shake table located at the University of Technology, Sydney. The table specifications are shown in Table 1.

Table 1 UTS shake table specifications

Size of table	3m x 3 m
Maximum Payload	10 tonnes
Overturning Moment	100 kN-m
Maximum Displacement	±100 mm
Maximum Velocity	±550 mm/sec
Maximum Acceleration	±2.5g or 0.9g (full load)
Testing Frequency	0.1 – 50 Hz

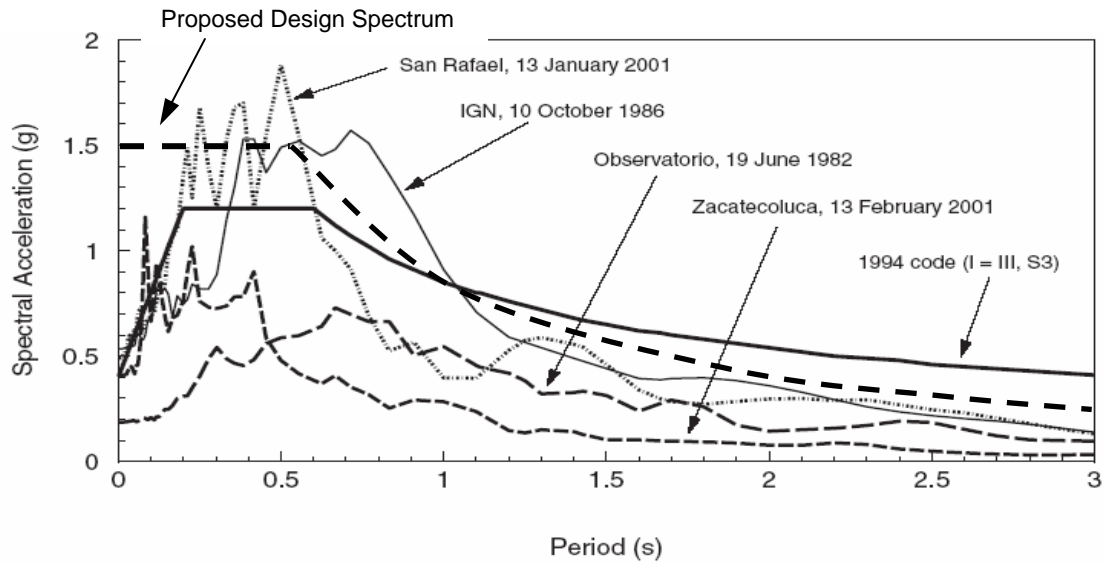


Figure 2. Proposed Design Spectrum (thick dashed line) vs Elastic Response Spectra developed from some El Salvador earthquakes (courtesy of Lopez et al. 2004)

5 DESCRIPTION OF INPUT TIME HISTORY FOR SHAKE TABLE SIMULATIONS

5.1 Proposed design spectrum

For seismic simulations using a shake table, an appropriate input time history signal is required. Selection and modification of a given input time history is based on the design response spectra recommended by relevant seismic standards. Since adobe structures generally exhibit an elastic response followed by a brittle failure mechanism, the Elastic Response Spectra was used in this study. The proposed design spectrum is a modified version of the El Salvador design spectrum (Fig. 2) reported by López et al (2004). Two modifications have been made to the El Salvador design spectrum as follows:

Elevation of spectral acceleration levels to better envelope recent and more severe earthquakes.

- Extension of the flat portion of the spectrum to a period of 0 seconds to cover a wider range of frequency contents (this is a conservative approach for very stiff structures).

The second modification is particularly important for masonry structures, which possess inherently higher resonant frequencies.

5.2 Selection and verification of input time histories

Once a suitable design spectrum has been chosen, the selection of an appropriate input time history can commence. The selection process includes calculating the Test Response Spectrum (TRS) for a given input time history and plotting it against the proposed design spectrum. Past earthquake re-

ords or artificially generated synthetic earthquakes can be used as the input time history. In this study, the input time history from the M_w 7.7 January 13, 2001 El Salvador earthquake was used. (This earthquake, in combination with a M_w 6.6 earthquake on February 13, 2001 in the same area, caused the destruction of over 110,000 adobe houses (DIGESTYC, 2001; Dowling, 2004a)). If the calculated TRS envelops the portion of the proposed design spectrum in the frequency range of interest, that particular input time history can be selected as the input signal for the shake table testing. Figure 3 shows the TRS vs the proposed design spectrum, in relation to frequency. It is only necessary that the proposed design spectrum be enveloped in the high frequency resonant range, which is typical of adobe wall units.

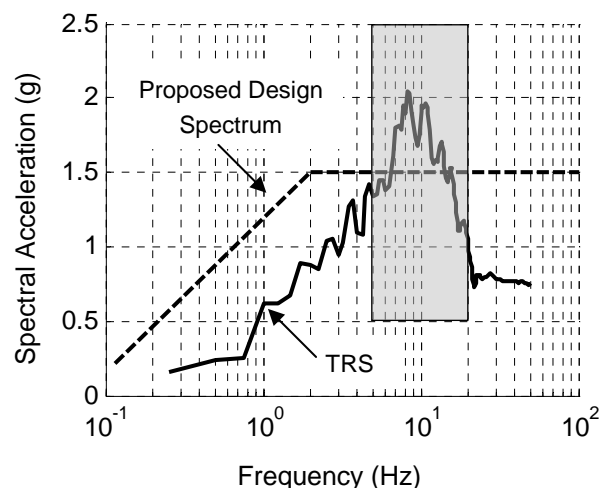


Figure 3. Calculated Test Response Spectrum (TRS) (solid line) in relation to the proposed design spectrum (dashed line). The shaded section is shown in Fig. 5.

5.3 Scaling of input time histories

In dynamic testing scaling often needs to be applied to retain dynamic similitude between different specimens. In other words, the frequency ratio, defined as the ratio of dominant input excitation frequencies to structural frequencies, should be similar for each specimen. This relationship between the natural frequency of the specimen and the dominant frequency range of the input spectrum determines the severity of response expected. If these frequencies are matched, resonance occurs, which produces the most damaging environment for the structure.

By means of modal analysis, the Frequency Response Function (FRF) of the scaled specimen was identified (Fig. 4), with the first resonant frequency (natural frequency) of around 29.6 Hz.

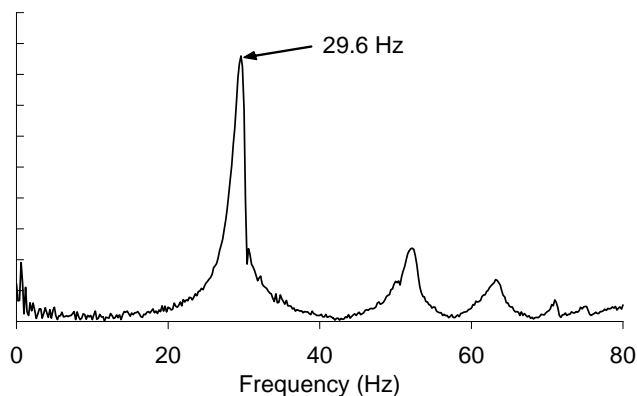


Figure 4. Frequency Response Function (FRF) of the specimen from the modal hammer tests.

Figure 5 shows the shaded section from Figure 3 and focuses on the frequency range of the Test Response Spectrum (TRS) in relation to the target maximum acceleration response of 1.5g (obtained from the proposed design spectrum). This figure reveals the dominant frequency range of the input spectrum (TRS) to be approximately 6.7 – 15.9 Hz. In order to assess the performance of the mudbrick specimens with respect to the proposed design spectrum (1.5g in the bandwidth of interest) a ‘target frequency zone’ (shaded circle) was identified. Given that the natural frequency of the specimen was 29.6 Hz, a scaling factor between 2.07 (29.6 Hz / 14.3 Hz) and 1.86 (29.6 Hz / 15.9 Hz) was necessary for proper dynamic similitude at the target acceleration. For simplicity, a scaling factor of 2.0 was applied in this case. The scaled input time history is shown in Figures 6 and 7.

The ‘target frequency zone’ between 14.3 and 15.9 Hz was selected in preference to the other option of 6.7 Hz which would have required a scaling factor of 4.4 (29.6 Hz / 6.7 Hz). Such a large scaling factor would have produced a very, very fast earthquake, with very small displacement and very high acceleration.

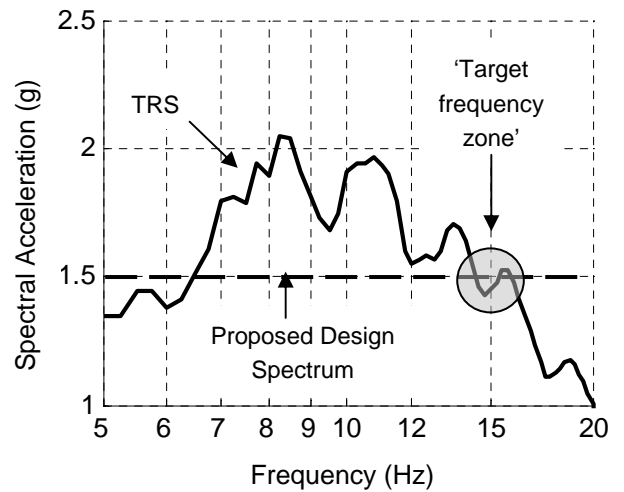


Figure 5. Test Response Spectrum (TRS) (solid line) in relation to the target maximum acceleration (1.5g)

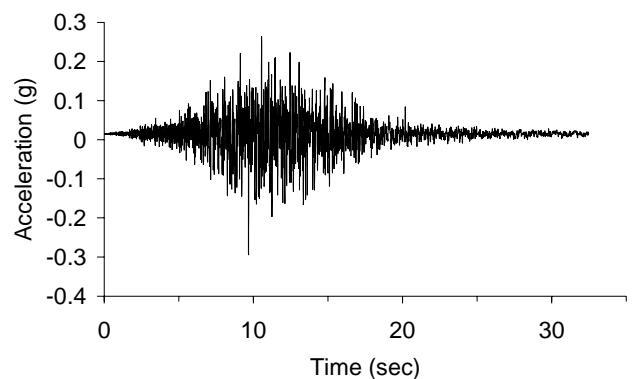


Figure 6. The scaled input time history (full)

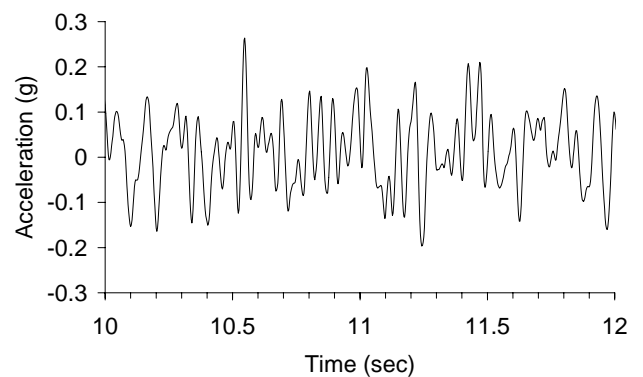


Figure 7. The scaled input time history (t = 10 to 12 sec)

6 RESULTS

The specimen exhibited four distinct and classic failure patterns. The initial and main failure was a large vertical crack in the NW corner, due to the large relative displacement between the in-plane shear ‘wing’ wall and the out-of-plane ‘long’ wall (Fig. 8). The crack was induced by tearing failure of both the mortar-brick interface and the individual brick units. The crack extended from the top of the wall to the base, with a maximum crack width of ~59 mm recorded during the experiment.



Figure 8. Large vertical crack in NW corner.

Another crack occurred in the NE corner, resulting from a similar failure mode (tearing failure between orthogonal walls). This crack did not propagate to the base of the wall, but linked with stair-step cracking in the ‘long’ wall (Fig. 9). This stair-step cracking can be attributed to the overturning of the ‘long’ wall, which was induced by the lack of connection with the western ‘wing’ wall, a result of the aforementioned vertical corner cracking.

The other crack was a vertical crack at the mid-span of the ‘long’ wall, which extended from the top of the wall to the intersection with the stair-step cracking (Fig. 9). It can be surmised that this crack was formed in a two-step process, consisting of a weakening stage and a failure stage.

Firstly, the flexure induced in the ‘long’ wall (prior to any vertical corner cracking) would have generated a splitting-crushing cycle at the mid-span section of the wall. Figure 10 shows the flexural displacement in the ‘long’ wall prior to formation of the first significant cracks in the specimen. Although both the recorded displacement data and the video footage fail to indicate whether notable cracking occurred at this location prior to the formation of the other cracks described above, it is clear that this process weakened the structure along this vertical plane, making it susceptible to damage by a secondary means.

After the failure of the corner connection between the ‘long’ wall and the western ‘wing’ wall, the wall panel experienced an overturning moment, with components about both the vertical and horizontal axes (out-of-plane). It seems reasonable to suggest that the moment generated about the vertical axis acted on the previously weakened vertical mid-span plane to cause cracking, with the width of crack larger at the internal face (splitting) than the external face (crushing) of the wall.



Figure 9. Internal view of wall unit showing stair-step and vertical cracking.

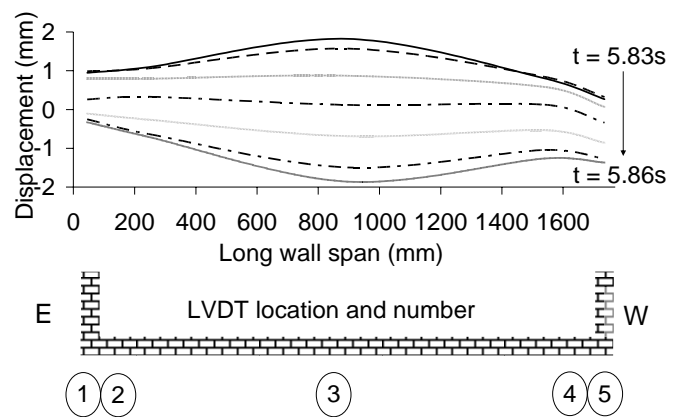


Figure 10. Flexural displacement of ‘long’ wall from $t = 5.83\text{s}$ to $t = 5.86\text{s}$ (prior to initial significant cracking)

The displacement-time history for LVDT 5 (western side of the ‘long’ wall) is shown in Figure 11. The time history graph shows the loss of stiffness of the specimen (an indication of major cracking) at $t \sim 6.2\text{s}$ and the significant offset of the sensor, with the post-failure neutral point $\sim 19\text{ mm}$ from the original (displacement = 0). The asymmetry of the specimen after failure is represented in the graph, with the largest displacements (negative displacements) occurring for wall motion outwards, and the ‘wing’ walls preventing large displacements inwards (positive displacement).

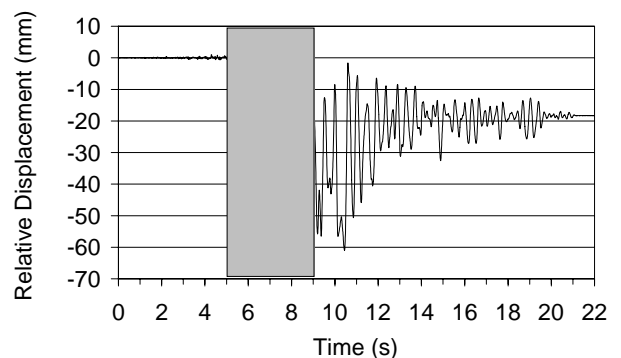


Figure 11. Displacement-time history for LVDT 5. (Shaded section is shown in Figure 12.)

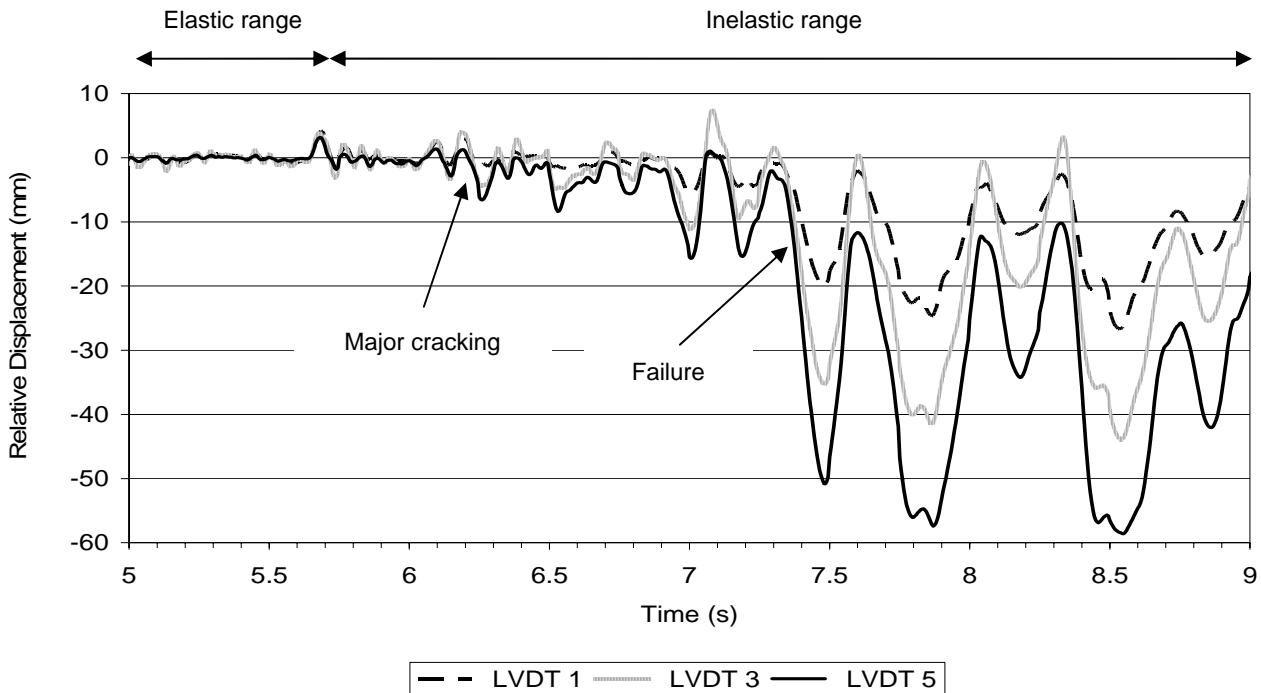


Figure 12. Displacement-time history for LVDTs 1, 3 and 5 (for $t = 5\text{ s}$ to $t = 9\text{ s}$).

Figure 12 shows an enlarged section of the time history. For the western section of the 'long' wall (recorded by LVDT 5) the elastic uncracked response is up to $t = \sim 5.7\text{ s}$, because the original neutral point (displacement = 0) is maintained. From $t = \sim 5.7\text{ s}$ the response can be considered inelastic (cracked phase). It is supposed that the initial cracking at the NW corner commenced at $t = \sim 6.2\text{ s}$, and failure of the corner occurred at $t = \sim 7.3\text{ s}$.

7 CONCLUSION

The test confirmed the destructive nature of ground motions containing sufficient energy and possessing dominant frequencies in the region of the natural frequencies of the wall unit. For these resonance conditions to occur, it may be necessary to modify the input time history spectrum, as done in this experiment. The u-shaped adobe wall panel displayed classic failure modes, indicative of damage to real houses subject to real earthquakes. This feature confirms that the selected specimen configuration, boundary conditions and test response spectrum are acceptable for this type of experiment. The establishment of these factors paves the way for future testing to determine the resistance capacity of specimens representing both traditional and improved structural systems.

8 REFERENCES

- DIGESTYC (Dirección General de Estadísticas y Censos). 2001. *Censo de viviendas afectadas por la actividad sísmica del año 2001*. San Salvador: DIGESTYC, Ministerio de Economía, El Salvador.
- Dowling, D.M. 2004a. *Adobe Housing Reconstruction after the 2001 El Salvador Earthquakes*. Oakland: Earthquake Engineering Research Institute (EERI).
- Dowling, D.M. 2004b. Adobe housing in El Salvador: Earthquake performance and seismic improvement. In Rose, W.I. et al. (eds), *GSA Special Paper 375: Natural Hazards in El Salvador: 281-301*. Geological Society of America.
- López, M., Bommer, J.J. & Pinho, R. 2004. Seismic hazard assessments, seismic design codes, and earthquake engineering in El Salvador. In Rose, W.I. et al. (eds), *GSA Special Paper 375: Natural Hazards in El Salvador: 301-320*. Geological Society of America.
- RESESCO (Reglamento Para la Seguridad Estructural de las Construcciones). 1997. *Folleto Complementario: Lineamiento para Construcción en Adobe*. San Salvador: Asociación Salvadoreña de Ingenieros y Arquitectos.
- U.S. Geological Survey. 2004. *Preliminary Earthquake Report: Southeastern Iran Dec 26, 2003*. Available on-line at http://neic.usgs.gov/neis/eq_depot/2003/eq_031226/ (Last accessed 22-4-04).
- Zegarra, L., Quiun, D., San Bartolomé, A. & Gisecke, A. 1997. *Reforzamiento de Viviendas de Adobe Existentes. Primera Parte: Ensayos Sísmicos de Muros 'U'*. Perú: Pontificia Universidad Católica del Perú.

Contact:

Bijan Samali: <bijan.samali@uts.edu.au>

Dominic Dowling: <dominic.m.dowling@uts.edu.au>

Jianchun Li: <jianchun.li@uts.edu.au>